1521-0111/12/8205-958–971$25.00
MOLECULAR PHARMACOLOGY
Vol. 82, No. 5
79848/3802950

Mol Pharmacol 82:958–971, 2012

LYG-202 Augments Tumor Necrosis Factor-α-Induced Apoptosis via Attenuating Casein Kinase 2-Dependent Nuclear Factor-κB Pathway in HepG2 Cells[S]

Fei-hong Chen, Na Lu, Hai-wei Zhang, Li Zhao, Li-cheng He, Hao-peng Sun, Qi-dong You, Zhi-yu Li, and Qing-long Guo

State Key Laboratory of Natural Medicines, Jiangsu Key Laboratory of Carcinogenesis and Intervention (F.C., N.L., H.Z., L.Z., L.H., Q.G.), and Department of Medicinal Chemistry (H.S., Z.L.), China Pharmaceutical University, Nanjing, China; and Jiangsu Center for Pharmacodynamics Research and Evaluation, Nanjing, China (Q.Y.)

Received May 4, 2012; accepted August 21, 2012

ABSTRACT

Tumor necrosis factor-α (TNF-α) is being used as an antineoplastic agent in treatment regimens of patients with locally advanced solid tumors, but TNF-α alone is only marginally active. In clinical use, it is usually combined with other chemical agents to increase its tumor response rate. Our previous studies reported that LYG-202 (5-hydroxy-8-methoxy-7-(4-(4-methylpiperazin-1-yl)butoxy)-2-phenyl-4*H*-chromen-4-one), a synthesized flavonoid with a piperazine substitution, has antiproliferative, antiangiogenic, and proapoptotic activities in multiple cancer cell lines. Here we evaluated the antineoplastic effect of TNF-α and analyzed the mechanism underlying its combination with LYG-202. Our results indicated that LYG-202 significantly increased the cytostatic and proapoptotic activity of TNF-α in HepG2 cells and heightened the protein level of apoptosis-related genes including caspase-3, caspase-8/9, cleaved poly(ADP-ribose) polymerase, and Bid. The fact that LYG-202 had a fitness score similar to that of the casein kinase 2 (CK2) inhibitor naphthyridine-8-carboxylate (CX-4945) implied to us that it may serve as a potential candidate for CK2 inhibitor, and the kinase activity assay suggested that LYG-202 significantly inhibited CK2 activity. Moreover, the electrophoretic mobility shift assay and luciferase assay showed that LYG-202 blocked the TNF-α-induced nuclear factor-κB (NF-κB) survival signaling pathway primarily by inactivating protein kinase CK2. In murine xenograft models, we also found that LYG-202 enhanced TNF-α antineoplastic activity and inhibited CK2 activity and NF-κB-regulated antiapoptotic gene expression. All these results showed that LYG-202 enhanced TNF-α-induced apoptosis by attenuating the CK2-dependent NF-κB pathway and probably is a promising agent in combination with TNF-α.

Introduction

Tumor necrosis factor-α (TNF-α) is a multifunctional cytokine playing roles in apoptosis, cell survival, inflammation, and immunity by triggering distinct signals (Wallach, 1997; Pfeffer, 2003; Balkwill, 2009). In several preclinical models and clinical trials, it exerts a direct cytotoxic effect to induce tumor regression and now serves as an antineoplastic agent for patients with locally advanced solid tumors (Egberts et al., 2008; Pilati et al., 2008). However, TNF-α alone shows only marginal activity, even with administration at high doses through local drug delivery systems. To increase ma-

This work was supported by the Project Program of State Key Laboratory of Natural Medicines, China Pharmaceutical University [Grant JKGZ201101]; the National Science and Technology Major Project [Grant 2012 ZX09304-001]; the National Natural Science Foundation of China [Grants 91029744, 21072232]; the Natural Science Foundation of Jiangsu Province [Grant BK2011620] and Program for Changjiang Scholars and Innovative Research Team in University [Grant PCSIRT-IRT1193]; the Talent Plan of Doctor Scholarship [Grant 2011 BPY06]; and the Graduate Education Innovation Project of Jiangsu Province [Grant CXZZ12_0324].

F.C. and N.L. contributed equally to this work.

Article, publication date, and citation information can be found at http://molpharm.aspetjournals.org.

http://dx.doi.org/10.1124/mol.112.079848.

[S] The online version of this article (available at http://molpharm.aspetjournals.org) contains supplemental material.

ABBREVIATIONS: TNF-α, tumor necrosis factor-α; TNFR1, TNF receptor 1; PARP, poly(ADP-ribose) polymerase; IκB, nuclear factor-κB inhibitory protein; IKK, IκB kinase; NF-κB, nuclear factor-κB; LYG-202, 5-hydroxy-8-methoxy-7-(4-(4-methylpiperazin-1-yl)butoxy)-2-phenyl-4*H*-chromen-4-one; CK2, casein kinase 2; MEKK, mitogen-activated protein kinase kinase kinase; MTT, 3-(4, 5-dimethylthiazol-2-yl)-2,5-diphenyltetrazolium bromide; PBS, phosphate-buffered saline; Z-VAD-FMK, *N*-benzyloxycarbonyl-Val-Ala-Asp(*O*-Met)-fluoromethyl ketone; CX-4945, 5-(3-chlorophenylamino benzo[c][2,6]naphthyridine-8-carboxylate; COX-2, cyclooxygenase-2; XIAP, X-linked inhibitor of apoptosis protein; MMP, matrix metalloproteinase; siRNA, small interfering RNA; DAPI, 4′,6-diamidino-2-phenylindole; FITC, fluorescein isothiocyanate; PI, propidium iodide; EMSA, electrophoretic mobility shift assay; CHIP, chromatin immunoprecipitation; PCR, polymerase chain reaction; PDB, Protein Data Bank; HCPT, 10-hydroxycamptothecin; TUNEL, TdT-mediated dUTP nick end labeling; ROS, reactive oxygen species.

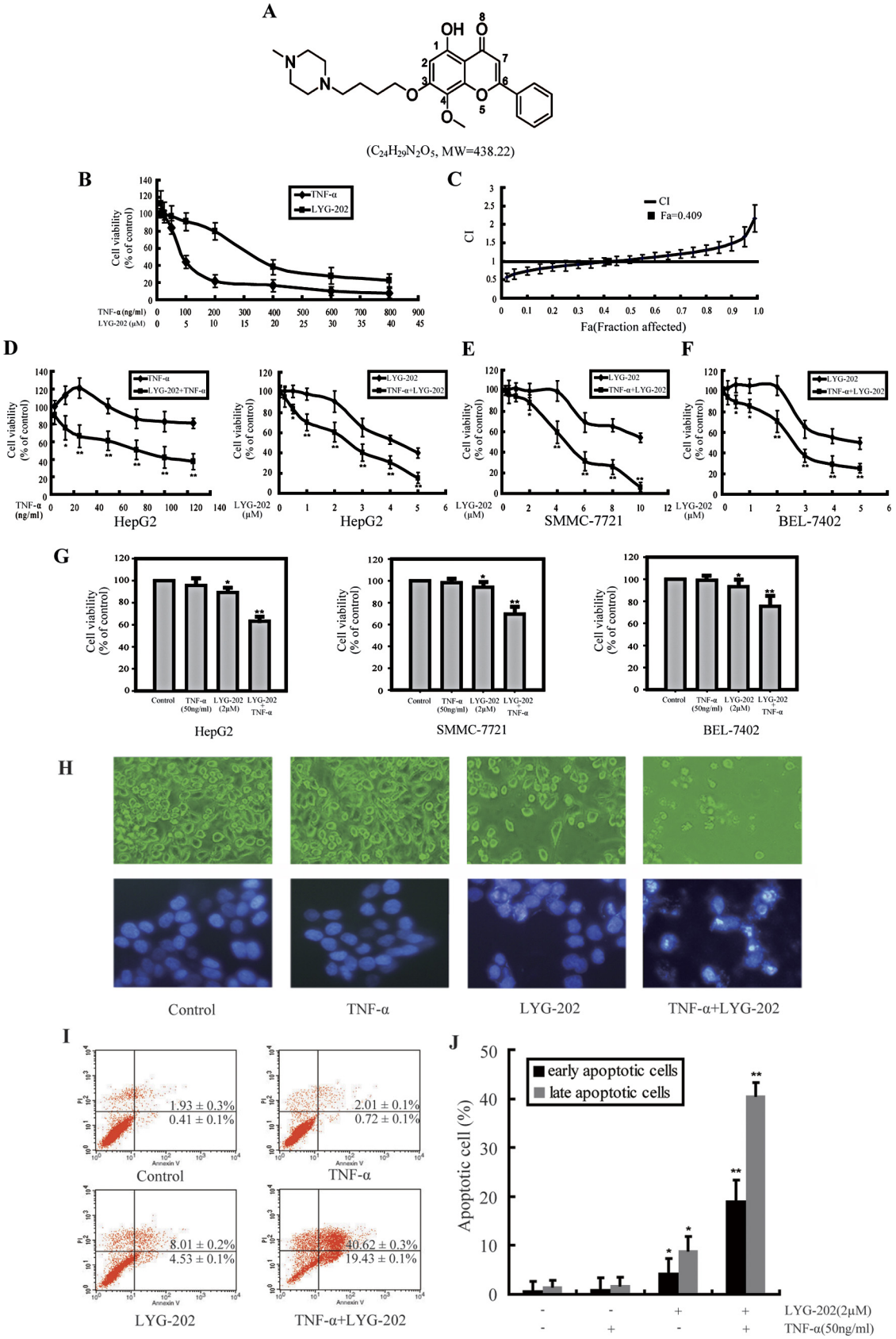

Fig. 1. LYG-202 accelerates TNF-α-induced apoptosis. A, molecular structure of LYG-202 [$C_{24}H_{29}N_2O_5$, molecular weight (MW) 438.22]. B, inhibitory effect of LYG-202 and TNF-α on cell proliferation in HepG2 cells. HepG2 cells were treated with various concentrations of LYG-202 or TNF-α alone for 24 h. Cell viability was determined by the MTT method. C, inhibitory effect and combination index of the combination treatment of LYG-202 and TNF-α. D, LYG-202 enhances TNF-α-induced cell growth inhibition in HepG2 cells. TNF-α slightly inhibits cell growth in a dose-dependent manner, and this inhibitory effect was significantly increased by 2 μM LYG-202 (left). In addition, LYG-202 inhibits cell growth in a dose-dependent manner

lignant cell sensitivity to TNF-α, it is combined with conventional antineoplastic agents (e.g., melphalan, paclitaxel, and actinomycin D) in clinical use (Manusama et al., 1996; de Wilt et al., 2000; Seynhaeve et al., 2002).

The majority of TNF-α biological activity is initiated via tumor necrosis factor receptor-1 (TNFR-1). TNF-α homotrimer binding to the extracellular domain of TNFR-1 induces TNFR-1 trimerization and releases the inhibitory protein silencer of death domains from TNFR-1 intracellular death domain and then recruits the adaptors including TNFR-associated death domain protein, Fas associated protein with death domain and caspase-8 and modulates caspase-9 and caspase-3. The activated caspase-8 and caspase-3 can induce Bid and PARP cleavage, respectively, and switch on cell apoptosis programs (Perez and White, 2000; Los et al., 2002). On the contrary, the bond also activates IκB kinase (IKK) and phosphorylates IκB, leading to its subsequent ubiquitination and proteasomal degradation, thereby allowing activated nuclear factor-κB (NF-κB) to translocate into the nucleus where it binds to specific sequences of DNA and activates the expression of some anti-apoptosis genes (Aggarwal, 2003; Sung et al., 2008), and the NF-κB signal is considered to be the major blocker in TNF-α-induced apoptosis. Thus, researchers explored agents that interfere with NF-κB survival pathway to reverse the resistance of both solid tumors and hematological malignancies to TNF-α (Uzzo et al., 2002; Braun et al., 2006) and improve the efficacy of apoptosis-inducing cancer therapies (Orlowski and Baldwin, 2002; Mocellin et al., 2005).

Flavonoids refer to a series of naturally occurring, low-molecular-weight plant products exhibiting a variety of biological activities such as antibacterial, antiviral, anti-inflammatory, antiallergic, and vasodilatory activities (Middleton et al., 2000; Nakamura et al., 2003; Suk et al., 2003). LYG-202 (5-hydroxy-8-methoxy-7-(4-(4-methylpiperazin-1-yl)butoxy)-2-phenyl-4*H*-chromen-4-one), a known synthesized flavonoid with a piperazine substitution (Fig. 1A), showed stronger antitumor effects than its parent compound (Zeng et al., 2009). Our previous studies showed that it has proapoptotic, antiproliferative, and antiangiogenic activities in vivo and in vitro (Zeng et al., 2009; Chen et al., 2010a,b; Liu et al., 2011). In the study, we investigated the effect of LYG-202 on NF-κB signaling and apoptosis in response to TNF-α. These results demonstrated that LYG-202 could augment TNF-α-induced apoptosis by blocking the NF-κB pathway. However, the exact molecular mechanism remains to be fully elucidated. Therefore, the inverse-docking approach was performed to screen potential protein targets of LYG-202 on the NF-κB pathway [e.g., casein kinase 2 (CK2), MEKK1, MEKK3, transforming growth factor β-activated kinase 1, and protein kinase Cθ].

CK2, a highly conserved and ubiquitous serine/threonine protein kinase that participates in the transduction of signals that promote cell growth and survival, plays a critical role in various steps of NF-κB signal activation induced by TNF-α (Litchfield, 2003). First, it activates IKKβ kinase and phosphorylates IκBα on Ser32/Ser36 and COOH-terminal proline-glutamic acid-serine-threonine residues (Schoonbroodt et al., 2000) and then phosphorylates the Rel A on Ser529, and this has a direct effect on the amplitude of transactivation (Wang et al., 2008). Hence, agents that can suppress CK2-induced NF-κB activation and enhance TNF-α-induced cell apoptosis could significantly improve the antitumor activity of TNF-α (Siddiqui-Jain et al., 2010).

In the present study, we evaluated the antineoplastic effect of TNF-α with or without LYG-202 in human hepatocellular carcinoma HepG2 cells, which are not sensitive to TNF-α (Sugimoto et al., 1999; Kusaba et al., 2007). Our results indicated that LYG-202 weakened CK2 activity and enhanced TNF-α-induced apoptosis by attenuating NF-κB signaling pathway in vitro and in vivo.

Materials and Methods

Materials. LYG-202 was synthesized by Dr. Zhiyu Li (China Pharmaceutical University, Nanjing, China), dissolved in dimethyl sulfoxide as a stock solution (10 mM) and stored at −20°C, and freshly diluted with RPMI 1640 medium (Invitrogen, Carlsbad, CA) to the final concentration. The control groups were always treated with dimethyl sulfoxide (0.1%, v/v). 3-(4,5-Dimethylthiazol-2-yl)-2,5-diphenyltetrazolium bromide (MTT) was obtained from Fluka Chemical Corp. (Ronkonkoma, NY) and dissolved in 0.01 M PBS. Recombinant human TNF-α was purchased from PeproTech (Rocky Hills, NJ), and recombinant mouse TNF-α was purchased from ProSpec-Tany TechnoGene Ltd. (Ness Ziona, Israel). Z-VAD-FMK (a caspase inhibitor) was purchased from Beyotime Institute of Biotechnology (Nantong, China). 5-(3-Chlorophenylamino benzo[*c*][2,6]naphthyridine-8-carboxylate (CX-4945) was obtained from Biochempartner Co. Ltd. (Shanghai, China). Primary antibodies of caspase-3, caspase-8, caspase-9, Bid, green fluorescent protein, Survivin, XIAP, c-Myc, MMP-9, p65, IκBα, phospho-IκBα, and β-actin were purchased from Santa Cruz Biotechnology, Inc. (Santa Cruz, CA). Antibodies against Bcl-2, Bcl-xL, and histones were obtained from Bioworld (St. Louis Park, MN). Antibodies against PARP, COX-2, and cyclin D1 were purchased from Cell Signaling Technology (Beverly, MA). Anti-CK2α/α' antibody was purchased from BD Biosciences (San Jose, CA). The plasmids of CK2α and CK2β were a kind gift from Dr. Stefania Sarno (University of Padova, Padova, Italy). CK2α siRNA was obtained from Santa Cruz Biotechnology, Inc.

Cell Lines and Cell Culture. The human hepatoma HepG2, SMMC-7721, and BEL-7402 cell lines, the mouse hepatoma H_{22} cell line, the liver L02 cell line, and the colon carcinoma HCT-116 cell line were originally obtained from the Cell Bank of Shanghai Institute of Cell Biology. HepG2 cells were cultured in RPMI 1640 medium supplemented with 10% heat-inactivated calf serum (Sijiqing). SMMC-7721, BEL-7402, and L02 cells were cultured in RPMI 1640 medium supplemented with 10% heat-inactivated fetal bovine serum (Sijiqing, Hangzhou, China). HCT-116 cells were cultured in McCoy's 5A supplemented with 10% heat-inactivated fetal bovine serum. All

in the presence of TNF-α at a nongrowth inhibitory dose (50 ng/ml) (right). Cell viability was analyzed by the MTT method. E and F, potentiation of TNF-α-induced cell growth inhibition in SMMC-7721 and BEL-7402 cells. Cell growth was analyzed by the MTT method. G, treatment effect of LYG-202 combined with TNF-α on cell proliferation in different hepatocellular carcinoma cell lines. The cells were pretreated with LYG-202 for 6 h and then incubated with TNF-α for 18 h. Cell growth was evaluated by the MTT method. H, LYG-202 enhances TNF-α-induced apoptosis. The cells were pretreated with 2 μM LYG-202 for 6 h and then incubated with 50 ng/ml TNF-α for 18 h. The morphology of HepG2 cells was observed under an inverted light microscope (400×), stained with DAPI reagent, and then analyzed under a fluorescence microscope (400×). I, cells pretreated with 2 μM LYG-202 for 6 h and then incubated with 50 ng/ml TNF-α for 18 h were examined by annexin V-PI double-staining assay. The *y*-axis shows the PI-labeled population and the *x*-axis shows FITC-labeled annexin V-positive cells. J, apoptotic rate of HepG2 cells caused by LYG-202, TNF-α, and their combination treatment. Values are means ± S.D. for at least three independent experiments performed in triplicate (*, $P < 0.05$; **, $P < 0.01$ compared with vehicle control).

media were also supplemented with 100 U/ml penicillin (Beyotime Institute of Biotechnology) and 100 μg/ml streptomycin (Beyotime Institute of Biotechnology) and maintained in a humidified atmosphere of 95% air/5% CO_2 at 37°C.

Animals. Male Kunming mice with body weight ranging from 18 to 22 g were provided by the animal facility at China Pharmaceutical University [No. SCXK (Su) 2002-0011]. Animals were maintained in a pathogen-free environment (23 ± 2°C; 55 ± 5% humidity) on a 12-h light/dark cycle with food and water supplied ad libitum throughout the experimental period.

Cell Viability Assay. Cells were plated at a density of 10^5 cells/ml per well in 96-well plates. After overnight growth, cells were exposed to medium containing LYG-202 for 6 h and then were treated with or without 50 ng/ml TNF-α for another 18 h at 37°C. Then cell viability was determined with the MTT method according to the previous description (Chen et al., 2010a).

Combined Effect Evaluation. Drug interaction between LYG-202 and TNF-α was assessed at a fixed concentration ratio of 1:1. The combination index (CI) was calculated as follows:

$$CI = (D)_1/(D_X)_1 + (D)_2/(D_X)_2$$

where $(D_X)_1$ and $(D_X)_2$ are the doses for LYG-202 and TNF-α in a combination that inhibits 50% cell growth, and $(D)_1$ and $(D)_2$ are the doses for each drug alone that inhibit 50% cell growth. CI <1, CI = 1, and CI >1 indicate synergistic, additive, and antagonistic effects, respectively (Chou, 2006). Data analysis was performed by CalcuSyn software (Biosoft, Oxford, UK).

Cell Morphology. HepG2 cells were seeded at 5×10^5 cells/well in six-well plates and grown for 24 h to attach themselves to the surface of the plates completely. In brief, cells were incubated with 2 μM LYG-202 for 6 h and then treated with or without 50 ng/ml TNF-α for another 18 h at 37°C, and a picture of live cells was taken under the inverted light microscope. In addition, their nuclei were photographed under a fluorescent microscope (IX51; Olympus, Tokyo, Japan) with a peak excitation wavelength of 340 nm after they were stained with DAPI as described previously (Zhang et al., 2010).

Apoptosis Assessment. The apoptosis induced by TNF-α alone or with LYG-202 was detected by an annexin V-FITC apoptosis detection kit (BioVision, Milpitas, CA) according to the manufacturer's protocol. In brief, cells were pretreated with 2 μM LYG-202 for 6 h and treated with 50 ng/ml TNF-α for 18 h. Then the cells were collected, resuspended in binding buffer (pH 7.5, 10 mM HEPES, 2.5 mM $CaCl_2$, and 140 mM NaCl), and incubated with annexin V-FITC and then with PI for 10 min in the dark at room temperature. Cells were analyzed by flow cytometry (FACSCalibur; BD, Franklin Lakes, NJ) and a computer station running CellQuest software (BD).

Western Blot Analysis. HepG2 cells were incubated with 2 μM LYG-202 for 6 h and then were treated with or without 50 ng/ml TNF-α for another 18 h at 37°C and collected. Western blot analysis for proteins was performed according to our previous methods (Chen et al., 2010b).

Electrophoretic Mobility Shift Assay. To assess the effect of LYG-202 on TNF-α-induced NF-κB activation, an electrophoretic mobility shift assay (EMSA) was performed with a chemiluminescent EMSA kit (Beyotime Institute of Biotechnology) following the manufacturer's protocol. In brief, nuclear extracts (5 μg/sample) were incubated with biotin-labeled oligonucleotides, 5′-AGT TGA **GGG GAC TTT CCC** AGG C-3′ and 3′-TCA ACT **CCC CTG AAA GGG** TCC G-5′ (boldface indicates NF-κB binding sites) in reaction buffers for 30 min at room temperature. The DNA-protein complex was separated from free oligonucleotide on 6% native polyacrylamide gels. The gels were visualized with a Bio-Rad infrared system and quantitated using Image Lab software (Bio-Rad Laboratories, Hercules, CA).

Cell Transfection and Luciferase Reporter Assay. The effect of LYG-202 on NF-κB-dependent reporter gene transcription induced by TNF-α was analyzed by luciferase reporter gene assays. HepG2 cells (5×10^5 cells/well) were plated in six-well plates and transfected transiently with the pNF-κB-luc plasmid (Beyotime Institute of Biotechnology) containing four NF-κB binding motifs (GGGAATTTCC) using Lipofectamine 2000 reagent (Invitrogen) according to the manufacturer's instruction. The pCDNA3.2 plasmid was added to make the total amount of DNA equal (4 μg/well in a six-well plate), and green fluorescent protein served as a normalization control. Then the cells were treated for 6 h with LYG-202 and stimulated with TNF-α (50 ng/ml) for another 18 h. Luciferase assays were performed with the Luciferase Reporter Gene Assay Kit (Promega, Madison, WI) and detected using Luminoskan Ascent (Thermo Fisher Scientific, Waltham, MA).

Chromatin Immunoprecipitation Assay. The CHIP assay was performed generally following the recommendations described previously with some modifications. HepG2 cells were incubated with 2 μM LYG-202 for 6 h and then treated with 50 ng/ml TNF-α for the indicated time. Cells were then cross-linked with formaldehyde, quenched with glycine, sonicated on ice, and centrifuged at 4°C. Mixtures were incubated with anti-p65 or preimmune IgG with rotation at 4°C overnight and then incubated with protein A+G agarose at 4°C for 6 h. Finally, immune complexes were captured by protein A+G agarose and eluted with elution buffer (1% SDS and 0.1 M $NaHCO_3$) at 37°C for 30 min. Cross-linking was reversed at 65°C for 4 h in a high salt buffer (0.2 M NaCl, 50 mM Tris, pH 6.5, 10 mM EDTA, and 0.2 mg/ml proteinase K). Extracted and dissolved immunoprecipitated DNA was quantified by real-time PCR with primers encompassing the NF-κB binding sites. Primers for COX-2 promoter quantification were 5′-TCT GGC GGA AAC CTG TGC GCT GG-3′ and 5′-AAA TTG CGT AAG CCC GGT GGG-3′ (forward and reverse, respectively) and for MMP-9 promoter quantification were 5′-CAG TGG AAT TCC CCA GCC TTG CCT-3′ and 5′-CCA CAC TCC AGG CTC TGT CCT C-3′. An equal volume of nonprecipitated (input) genomic DNA was used to correct for the differences in PCR amplification efficiencies and amounts of DNA. The PCR analyses were performed with a real-time PCR kit (TaKaRa Biotechnology Co. Ltd., Dalian, China).

Immunocytochemical Localization of NF-κB/p65 Subunit. The effect of LYG-202 on the nuclear translocation of p65 was examined by immunocytochemical analysis as described previously. In brief, cells were pretreated with 2 μM LYG-202 for 6 h after being seeded on a gelatin-coated glass, after stimulation with or without 50 ng/ml TNF-α for 30 min, fixed with 4% paraformaldehyde, and permeabilized with 0.2% Triton X-100. After being washed with PBS, the fixed cells were blocked with 3% bovine serum albumin for 1 h and then incubated with rabbit polyclonal anti-p65 antibody (1:50) overnight at 4°C, washed with PBS and incubated with anti-rabbit IgG-FITC (1:100) for 1 h, and counterstained for nuclei with the fluorochrome dye DAPI (Santa Cruz Biotechnology, Inc.). Stained slides were observed under a fluorescence microscope (Olympus) with a peak excitation wavelength of 340 nm.

IKKβ Activity Assay. The effect of LYG-202 on IKKβ activity was determined using the HTScan IKKβ kinase assay kit (Cell Signaling Technology) as described previously (Sun et al., 2010).

Molecular Docking. We used our protein-ligand docking software package GOLD to dock LYG-202 into many potential drug targets that could activate IKKβ activity (Hayden and Ghosh, 2004; Schmid and Birbach, 2008). Molecular docking was performed following the method of Sun et al. (2010). We then ranked each protein according to the GOLD fitness score. Inhibitors of the top targeted protein were considered to have effects on TNF-α-induced apoptosis similar to LYG-202, which could be detected in the biological test. Previous studies showed that the binding site was defined by analyzing the protein-ligand interactions of cocrystal structures that were deposited in PDB (http://www.rcsb.org/pdb). Molecular interactions were observed using Discovery Studio (Accelrys, San Diego, CA). In the study, LYG-202 was detected for its interaction with major binding sites of selected proteins.

CK2 Activity Assay. CK2 activity after treatment with TNF-α alone or in combination with LYG-202 was detected with the CK2

assay kit (MBL International, Woburn, MA) according to the manufacturer's instruction (Sun et al., 2010).

Down-Regulation of CK2 by siRNA. HepG2 cells were plated at 5×10^5 cells/well in six-well plates and allowed to adhere for 24 h. siRNA transfections were performed according to the manufacturer's instructions for Lipofectamine 2000 reagent. After that, HepG2 cells preincubated with 2 μM LYG-202 for 6 h and then treated with or without 50 ng/ml TNF-α for another 18 h at 37°C were recovered and used for appropriate determinations.

Real-Time PCR Analysis. Total RNA was extracted using TriPure Isolation Reagent (Roche Diagnostics, Mannheim, Germany) and then were amplified by PCRs. The primer sets used in the PCR amplification were as follows: for CK2α, forward 5′-TCA CAG CAG CAT GGG AAT TAT GCA C-3′ and reverse 5′-AGC AAC TCG GAC ATT ATA TTC TTG G-3′. The relative expression of CK2α was analyzed using quantitative RT-PCR with glyceraldehyde-3-phosphate dehydrogenase as an internal control as described previously (Lu et al., 2012).

Murine Xenograft Tumor Assay. Murine hepatoma 22 (H_{22}) cells were diluted with ice-cold 0.9% saline and inoculated subcutaneously at the right axilla of mice (5×10^6 viable cells/ml) (Wang et al., 2008; Zhao et al., 2010). Twenty-four hours after inoculation, mice were divided randomly into 11 groups (with 10 mice/group): saline tumor control group; TNF-α 1.5 μg/day group; LYG-202 750, 500, 250, and 125 mg/kg; LYG-202 750, 500, 250, and 125 mg/kg + TNF-α combination group; and 10-hydroxycamptothecin 30 mg/kg group. Mice were administered LYG-202 or 10-hydroxycamptothecin orally and TNF-α by subcutaneous injections, which were given once every 2 days. From the 3rd day after treatment, the tumors were measured continuously. Tumor volume (TV) was calculated using the formula

$$\text{TV } (\text{mm}^3) = d^2 \times D/2;$$

where d and D are the shortest and the longest diameter, respectively.

At the 7th day after treatment, the mice were sacrificed, and tumors were ablated carefully and weighed after any remaining blood was washed off with PBS. The tumor inhibitory ratio was calculated by the formula

$$\text{Tumor inhibitory ratio } (\%) = [(W_{\text{Control}} - W_{\text{Treated}})/W_{\text{Control}}] \times 100\%$$

where W_{Treated} and W_{Control} are the average tumor weights of the treated and control mice, respectively. This study was approved in the SPF animal laboratory of China Pharmaceutical University.

The coefficient of drug interaction (CDI) was used to analyze effects of drug combinations (Cao and Zhen, 1989). CDI is calculated as follows:

$$\text{CDI} = AB/(A \times B).$$

According to the tumor weight of each group, AB is the ratio of the combination groups to control group, and A or B is the ratio of the single agent group to the control group. When CDI = <1, synergism is indicated. When CDI = 1, summation is indicated. When CDI = >1, antagonism is indicated. CDI = <0.75 indicates that the drugs are significantly synergistic.

Histology. Hepatoma tumors were fixed in 10% formalin and processed routinely for paraffin embedding. Tissue sections were prepared with a microtome and placed on glass slides. A TUNEL assay was performed to detect apoptotic cells using a TUNEL detection kit (KeyGEN, Nanjing, China) according to the manufacturer's instructions.

Statistical Analyses. All quantitative data are presented as the mean ± S.D. from at least three samples per data point. Statistical analyses were performed using an unpaired, two-tailed Student's t test. All comparisons are made relative to untreated controls, and significance of difference is indicated as *, $P < 0.05$ and **, $P < 0.01$.

Results

LYG-202 Enhances TNF-α-Induced Growth Inhibition and Apoptosis. The inhibitory effects of LYG-202 and TNF-α on cell viability in HepG2 cells were assessed after incubation with increasing concentrations of LYG-202 and TNF-α for 24 h. Results indicated that LYG-202 and TNF-α showed an inhibitory effect in a concentration-dependent manner (Fig. 1B), and the IC_{50} of LYG-202 and TNF-α was 262.02 ± 12.52 ng/ml and 5.98 ± 0.65 μM, respectively. To investigate the inhibitory effect of the combination treatment, cells were exposed to LYG-202 for 6 h and then incubated with TNF-α for 18 h at a fixed ratio (LYG-202 IC_{50}/TNF-α IC_{50} ratios were 1:1) (Chou, 2006). Data in Fig. 1C show that the CI values were <1 when the values of fraction affects (Fa) were smaller than 0.409 (at the point at which the concentration of LYG-202 and TNF-α was approximately 2.05 μM and 88.91 ng/ml, respectively), which indicated that the combination of TNF-α and LYG-202 exerted a synergistic inhibitory effect on cell proliferation in HepG2 cells at concentrations smaller than the threshold values (drug concentrations when CI = 1).

To further determine the effect of LYG-202 on TNF-α-induced growth inhibition of HepG2 cells, we treated HepG2 cells with different concentrations of TNF-α or LYG-202 alone or in combination. Our results indicated that treatment with TNF-α alone had little effect on the growth of HepG2, but there was a moderate inhibitory effect with LYG-202 alone, and in the presence of a moderate inhibitory dose of TNF-α (50 ng/ml) or LYG-202 (2 μM), the combination was highly effective on HepG2 cell growth (Fig. 1D). Similar effects were observed in SMMC-7721 (Fig. 1E) and BEL-7402 cells (Fig. 1F).

The cell viability with TNF-α alone (50 ng/ml), LYG-202 alone (2 μM), and the combination was 98.3, 95.6, and 65.5%, respectively, in HepG2 cells. These results suggested the significant synergy of TNF-α and LYG-202 on the inhibition of HepG2 cell proliferation. Similar results were also found for the combination of LYG-202 with TNF-α in different hepatocellular carcinoma cell lines (Fig. 1G).

Then we analyzed the effect of LYG-202 on TNF-α-induced apoptosis, which is one of the major ways for cell death (Bosman et al., 1996), with DAPI and annexin V-PI double staining. Results indicated that the live cells were obviously decreased (Fig. 1H, top row), and the number of cells in which the chromatins condensed increased (Fig. 1H, bottom row). Moreover, annexin V-PI double-staining analysis indicated that LYG-202 potentiated TNF-α-induced early apoptosis from 0.72 to 19.43% and late apoptosis strikingly from 2.01 to 40.62% (Fig. 1, I and J), suggesting a synergistic effect of LYG-202 with TNF-α in inducing cell apoptosis.

LYG-202 Potentiated TNF-α-Induced Caspase Activation and Bid and PARP Cleavage in HepG2 Cells. To understand the role of caspases in TNF-α-mediated apoptosis with or without LYG-202, Western blotting was performed. We found that TNF-α alone had a minimal effect on the protein level of cleavage of caspase-8 and -3/9 and their activated form, and no effect on procaspase-8 and -3/9. In the presence of LYG-202, however, the cleaved products markedly accumulated, whereas the level of procaspase-8 and -3/9 decreased in a time-dependent manner (Fig. 2A).

Bid is a specific proximal substrate of caspase-8, and cleavage of both is a feature of TNF-α lethality (Li et al., 1998; Perez and White, 2000). The proteolytic cleavage of PARP, a substrate of caspase-3, has been considered to be a hallmark of apoptosis (Los et al., 2002). Therefore, the cleavages of Bid

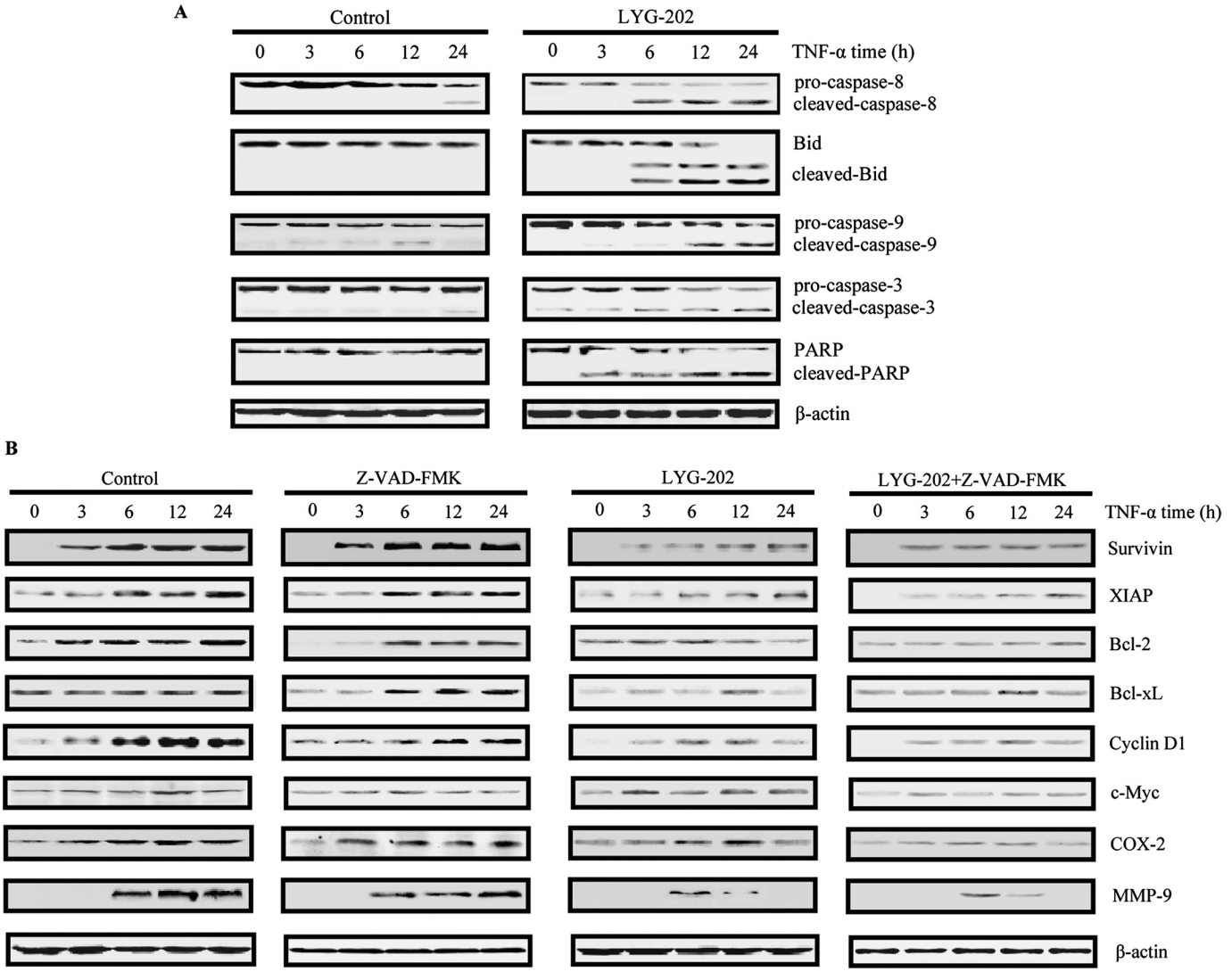

Fig. 2. LYG-202 potentiated TNF-α-induced caspase activation and suppressed NF-κB-regulated gene expression. HepG2 cells were treated with 2 μM LYG-202 for 6 h and then incubated with 50 ng/ml TNF-α for the indicated times. A, augmentation of TNF-α-induced caspase activation and Bid and PARP cleavages by LYG-202. Whole-cell extracts were prepared and analyzed by Western blot using the antibodies indicated. B, LYG-202 represses TNF-α-induced NF-κB-dependent expression of antiapoptosis-related (Survivin, XIAP, Bcl-2, and Bcl-xL), proliferation-related (cyclin D1, c-Myc, and COX-2), and metastasis-related (MMP-9) gene products in the absence and presence of 20 μM Z-VAD-FMK. The results shown are representative of three independent experiments.

and PARP were also tested. Western blot analysis suggested that neither TNF-α nor LYG-202 alone had an effect on Bid and PARP cleavage, but together they were very effective in inducing cleavages of Bid and PARP (Fig. 2A). These results indicated that LYG-202 can facilitate the activation of caspase and cleavages of Bid and PARP in the TNF-α-induced apoptotic pathway.

LYG-202 Suppressed the Expression of NF-κB-Regulated Gene Products in HepG2 Cells. We know that TNF-α triggers both the caspase-protease pathway and the NF-κB pathway, and the balance of these two pathways is critical for the ultimate fate of a cell: death or survival (Brown et al., 2010). These findings prompted us to determine whether LYG-202 could enhance TNF-α-induced apoptosis by attenuating the NF-κB pathway.

To examine the effect of LYG-202 on the NF-κB pathway, we analyzed the expression of its downstream genes involved in antiapoptosis (Survivin, XIAP, Bcl-2, and Bcl-xL), proliferation (cyclin D1, COX-2, and c-Myc), and invasion (MMP-9). As shown in Fig. 2B, in the absence of LYG-202, TNF-α induced the expression of survival and invasion genes including Survivin, XIAP, Bcl-2, COX-2, and MMP-9 in a time-dependent manner. Of interest, the level of cyclin D1 and c-Myc increased for the first 12 h but decreased at 24 h, whereas that of Bcl-xL showed little change. However, in the presence of LYG-202, the increase in these gene expressions was weakened and even reversed. Pretreatment with Z-VAD-FMK, a caspase inhibitor, barely blocked the down-regulation of NF-κB-mediated gene expression, suggesting that the down-regulation of various target proteins was not caspase-dependent and may be upstream of the apoptotic pathway. These results indicated that LYG-202 inhibited the target gene expression of NF-κB, implying that it facilitated TNF-α-induced apoptosis by blocking NF-κB signaling.

LYG-202 Inhibited TNF-α-Dependent NF-κB Activation in HepG2 Cells. To further understand the role of NF-κB in TNF-α-induced apoptosis of HepG2 cells treated with LYG-202, the DNA-binding activity of the NF-κB com-

plex in nuclear extracts was evaluated by EMSA. As shown in Fig. 3, LYG-202 alone had a minimal effect on NF-κB activation at different doses and time courses (Fig. 3A, left column), whereas it significantly inhibited TNF-α-induced NF-κB activation in dose- and time-dependent manners (Fig. 3A, right column).

LYG-202 Repressed TNF-α-Activated NF-κB-Dependent Gene Transcription. To determine the effect of LYG-202 on NF-κB-dependent gene transcription directly, a p65-luciferase reporter gene assay was performed. Results indicated that LYG-202 inhibited TNF-α-induced p65 reporter gene activity in a dose-dependent manner (Fig. 3B).

To further confirm these data, we performed a CHIP assay to test the activity of NF-κB binding to promoters of COX-2 and MMP-9, two NF-κB target genes. Results showed that TNF-α induced this activity in a time-dependent manner, whereas LYG-202 abolished it (Fig. 3C).

These findings suggested that LYG-202 strongly inhibited TNF-α-induced NF-κB-dependent gene transcription by interfering with the binding of NF-κB to its target gene promoters in HepG2 cells.

LYG-202 Inhibited TNF-α-Induced Nuclear Translocation of p65. The nucleus localization of p65, a subunit of the NF-κB complex, is essential for the transcriptional activity of NF-κB (Mocellin et al., 2005), so nuclear and cytoplasmic extracts were obtained to examine the nuclear translocation of p65. Results showed that TNF-α-induced nuclear translocation of p65 was detected in 15 min and lasted for more than 1 h (Fig. 4A, left column), whereas it was inhibited by LYG-202 (Fig. 4A, right column). Similar data were also observed in the immunofluorescence assay (Fig. 4B). These results suggested that LYG-202 interferes with TNF-α-induced p65 (a subunit of NF-κB) nuclear translocation in HepG2 cells.

LYG-202 Inhibited TNF-α-Mediated IκBα Phosphorylation and Degradation and IKKβ Activity. NF-κB activates the transcription of target genes by binding with a consensus sequence in the nucleus, and the translocation of NF-κB to the nucleus is preceded by the phosphorylation, ubiquitination, and proteolytic degradation of IκB (Karin and Ben-Neriah, 2000). We determined whether LYG-202 inhibitory activity was due to inhibition of IκBα phosphorylation

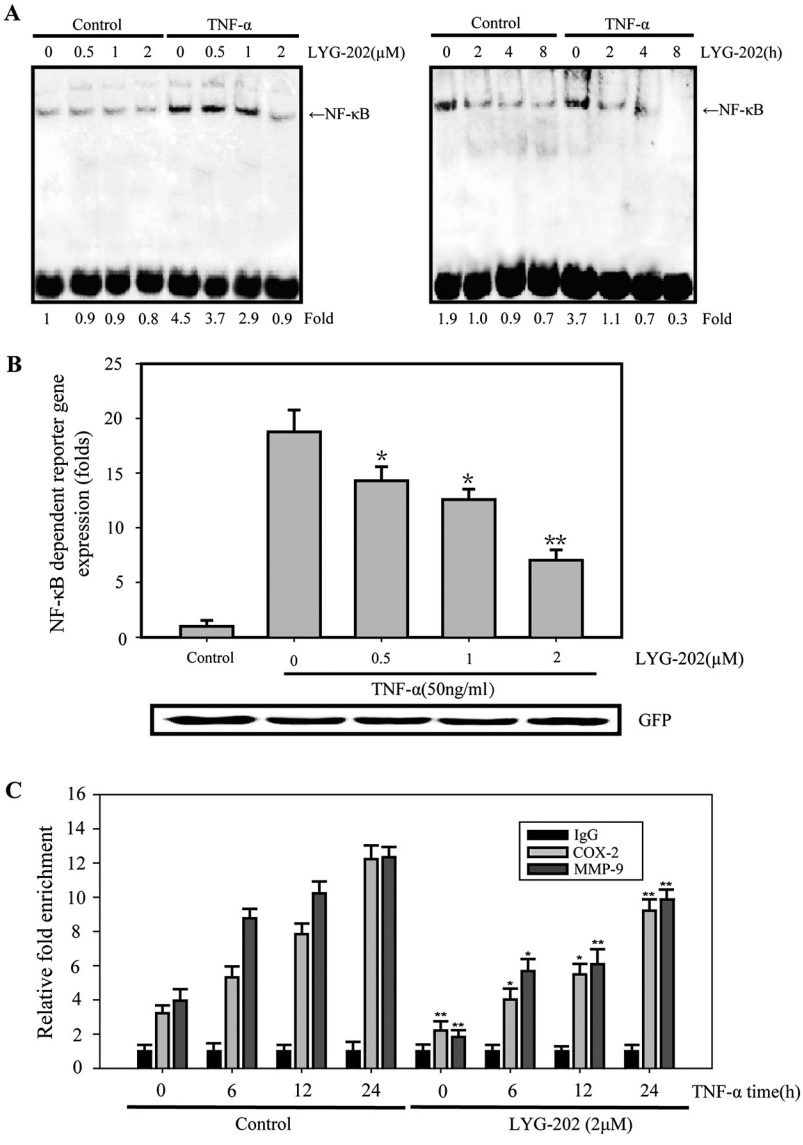

Fig. 3. LYG-202 inhibited TNF-α-induced NF-κB activation. A, dose- and time-dependent effect of LYG-202 on TNF-α-induced NF-κB activation. HepG2 cells were pretreated with LYG-202 at the indicated concentrations and time and incubated with 50 ng/ml TNF-α for 30 min and then subjected to EMSA to test for NF-κB activation. B, LYG-202 inhibited TNF-α-induced NF-κB-dependent reporter gene expression. HepG2 cells were transiently transfected with a NF-κB luciferase reporter gene. After transfection, cells were pretreated with the indicated concentrations of LYG-202 for 6 h and then were incubated with 50 ng/ml TNF-α for an additional 18 h. Cell supernatants were collected and assayed for luciferase activity as described. C, LYG-202 inhibited the binding of NF-κB to the COX-2 and MMP-9 promoters. HepG2 cells were pretreated with 2 μM LYG-202 for 6 h and treated with 50 ng/ml TNF-α for the indicated times. The proteins were cross-linked with DNA by formaldehyde and then subjected to CHIP assay using an anti-p65 antibody with the COX-2 and MMP-9 primers. Values are means ± S.D. for at least three independent experiments performed in triplicate (*, $P < 0.05$; **, $P < 0.01$, compared with HepG2 cells treated with TNF-α). GFP, green fluorescent protein.

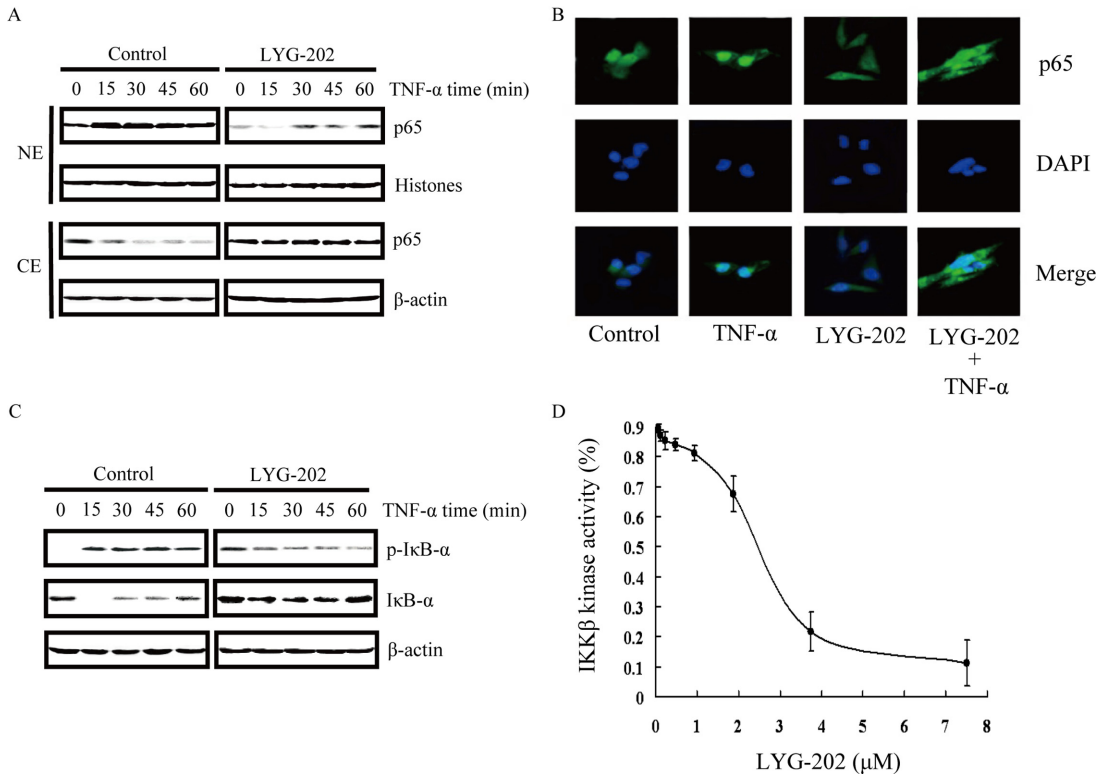

Fig. 4. LYG-202 inhibits TNF-α-mediated p65 nuclear translocation, IκBα phosphorylation and degradation, and IKKβ activation. A, effect of LYG-202 on TNF-α-induced p65 nuclear translocation. Cells were incubated with 2 μM LYG-202 for 6 h and treated with 50 ng/ml TNF-α for the indicated times. Cytoplasmic extracts (CE) and nuclear extracts (NE) were prepared, fractionated on SDS-polyacrylamide gel electrophoresis, and electrotransferred to nitrocellulose membrane. Western blot analysis was performed using the antibodies indicated. B, immunofluorescence analysis of p65 localization. Cells were incubated with 2 μM LYG-202 for 6 h and then treated with 50 ng/ml TNF-α for 30 min. Cells were subjected to immunocytochemical analysis. C, effect of LYG-202 on the phosphorylation and degradation of IκBα by TNF-α. Cells were preincubated with 2 μM LYG-202 for 6 h and then were treated with 50 ng/ml TNF-α for 30 min. Cytoplasmic extracts were fractionated and then subjected to Western blot analysis using the anti-IκBα and anti-p-IκBα antibodies. D, LYG-202 inhibits exogenous IKKβ activity. The results shown are representative of three independent experiments.

and degradation. Western blot analysis indicated that TNF-α induced the phosphorylation of IκBα within 15 min, whereas LYG-202 at 2 μM blocked its phosphorylation (Fig. 4C, top row) and suppressed its degradation induced by TNF-α (Fig. 4C, middle row).

The facts that TNF-α-induced IκBα phosphorylation requires IKKβ (Hayden and Ghosh, 2004; Böcker et al., 2008; Schmid and Birbach, 2008) and is inhibited by LYG-202 prompted us to determine the effect of LYG-202 on IKKβ activation. Results from the IKKβ kinase assay showed that LYG-202 obviously suppressed IKKβ activity in a dose-dependent manner (Fig. 4D). These results demonstrate that LYG-202 inhibited TNF-α-induced IκBα phosphorylation and degradation and IKKβ activity.

Docking Analysis. After docking LYG-202 to each structure of the PDB, we ranked 11 target proteins that could activate IKKβ activity according to the GOLD fitness score (Table 1). Among these proteins, the crystal structure of human CK2 holoenzyme (PDB code 1ZOG) was the highest-ranked human protein with a fitness score of 47.8621, compared with the similar score of 48.2899 for the potent CK2 inhibitor CX-4945 (Pierre et al., 2011; Siddiqui-Jain et al., 2010). The results demonstrated that CX-4945 could enhance TNF-α-induced apoptosis (Supplemental Fig. 1B) and inhibit NF-κB activation (Supplemental Fig. 1C). These effects of CX-4945 are similar to the corresponding characteristic effects of LYG-202, implying that CK2 may be a promising target of LYG-202 in blocking NF-κB signaling activation.

Previous studies showed that the binding site was defined by analyzing the protein-ligand interactions of all 23 CK2 cocrystal structures that were deposited in PDB. All the ligands in the complex structures showed hydrophobic interactions with Val53, Val66, and Ile174, which play a crucial role in CK2 inhibition. In addition, Arg47, Lys68, Phe113, Val116, Asn118, Met163, and Asp175 are also very important in the binding interactions of CK2 and its ligands. A docking study showed that LYG-202 formed two hydrogen bonds with Asp175 and Asn118, the two key residues located in the polar region and hinge region, respectively, which were essential for CK2 activity. In addition, LYG-202 showed a favorable hydrophobic interaction with ARG43 in the binding pocket of CK2 (Fig. 5A). The results indicated that LYG-202 could be considered to be a novel CK2 inhibitor that should be confirmed in the further biological tests.

Effect of LYG-202 on TNF-α-Induced CK2 Activity. Protein kinase CK2 is a Ser/Thr kinase involved in various steps of the TNF-α-induced NF-κB activation process. We investigated whether LYG-202 directly inhibits TNF-α-induced CK2 activity. Results from the CK2 kinase assay demonstrated that TNF-α induced the activation of CK2, and LYG-202 suppressed TNF-α-mediated CK2 activity compared with CX-4945 (Fig. 5B). Neither TNF-α nor LYG-202 affected the expression of CK2 protein subunits (Fig. 5C).

Transfection of Protein Kinase CK2 Reverses the Effect of LYG-202. It was reported that CK2 could modulate IKKβ-mediated phosphorylation IκB (Yu et al., 2006). Molec-

TABLE 1

The 11 kinase structures upstream of IKKβ activation targeted by LYG-202 according to inverse docking

LYG-202 was docking to the structures from the PDB. The kinase structures with the most favorable docking scores are listed in descending order. The GOLD score fitness of the CK2 inhibitor CX-4945 is 48.2899 with PDB code 1JWH.

PDB Identification	Kinase	Score	Rank
1ZOG	CK2	47.8621	1
1HE8	PI3K	39.0231	2
3EQF	MEKK1	38.9389	3
2EVA	TAK1	34.8353	4
3CQW	AKT	32.9431	5
2DYL	MAP3K7	31.5247	6
1F3V	TRAF2	27.3698	7
1XLD	PKCθ	26.9243	8
3V55	MALT1	26.5272	9
2G5X	RIP1	25.8782	10
2PPH	MEKK3	22.9584	11

PI3K, phosphatidylinositol 3-kinase; TAK1, transforming growth factor β-activated kinase 1; MAP3K7, mitogen-activated protein kinase kinase kinase 7; TRAF2, TNFR-associated factor 2; PKCθ, protein kinase Cθ; MALT1, mucosa-associated lymphoid tissue lymphoma translocation protein 1.

ular docking analysis showed that LYG-202 had hydrogen bonds with Asp175 and Asn118, which were essential for CK2 activity (Sun et al., 2010), in the binding pocket of CK2; moreover, it inhibited TNF-α-induced CK2 activity but had no effect on its expression (Fig. 5, B and C).

To explore the potential role of CK2 in NF-κB suppression induced by LYG-202, we detected the expression of CK2 in L02, HepG2, and HCT116 cell lines and transiently transfected CK2α (the catalytic subunit) and CK2β (the regulatory subunit) into cells to determine whether the elevated CK2 activity affects the activity of LYG-202. The results in Fig. 6A show that the expression of CK2 in L02 and HepG2cells is lower than that in HCT116 cells with a known high CK2 protein level, suggesting that we can transfect the HepG2cells with CK2α /CK2β plasmids to increase CK2α activity.

As shown in Fig. 6B, transfection of either CK2α or CK2β subunits or both gives rise to the expected patterns with the anti-Myc antibody. A 75, 20, and 102% increase in CK2 activities from HepG2 cells that were transfected with CK2α, CK2β, and both was observed compared with the control (Fig. 6C). Results in Fig. 6D shown that the IKKβ kinase activity showed little change in cells transfected with CK2β alone, but transfection of CK2α or both led to 30 and 54% increases in IKKβ kinase activities. These data provide evidence that both are required for NF-κB activation. In the following experiment, both of them were transfected to activate NF-κB.

We tested the effect of LYG-202 on NF-κB-dependent gene transcription and TNF-α-induced apoptosis in the absence or presence of CK2α and CK2β. Data indicated that the cotransfection of these two subunits reversed, at least partially, the inhibitory effect of LYG-202 on TNF-α-induced NF-κB-dependent gene transcription (Fig. 6E), consequently diminishing the effect of LYG-202 on TNF-α-induced apoptosis (Fig. 6, F and G). These results implied that CK2 was involved in LYG-202 suppression of TNF-α-induced NF-κB activation in HepG2 cells. The results in Supplemental Fig. 2A show that CK2 siRNA down-regulated the mRNA of CK2 by nearly 75%

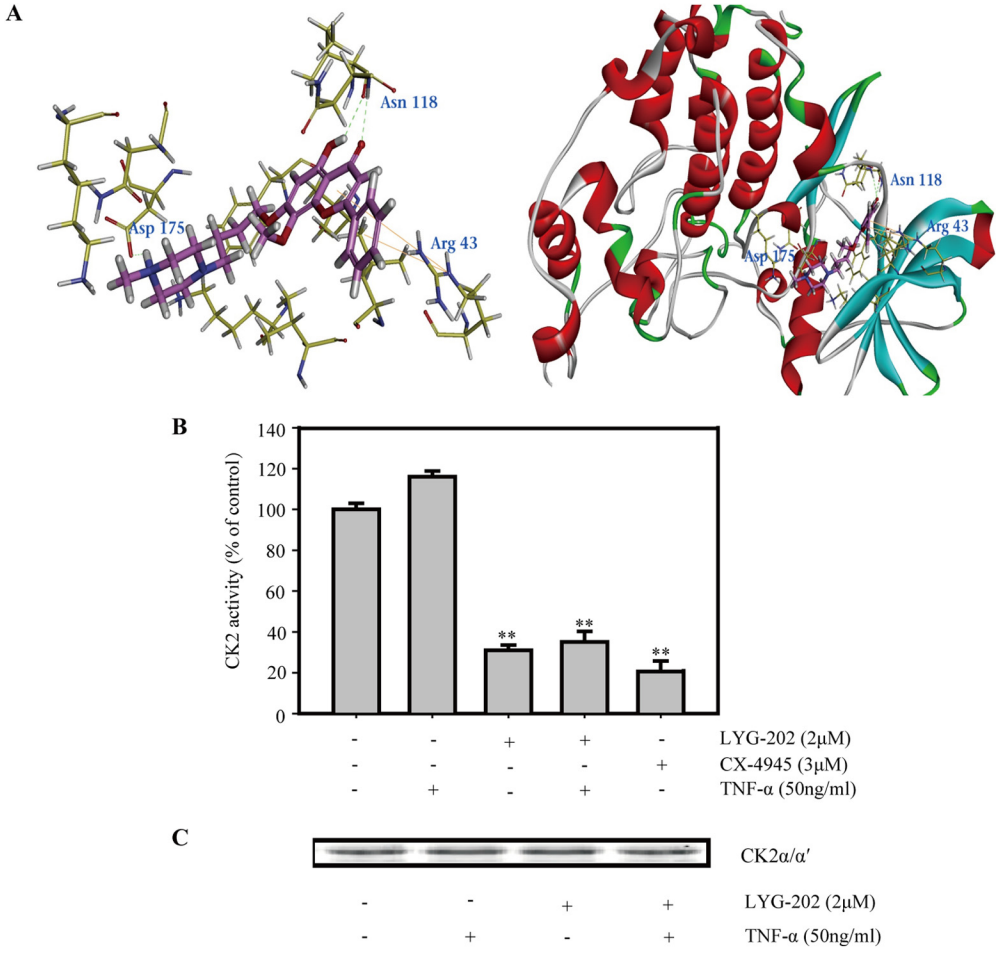

Fig. 5. LYG-202 reduced TNF-α-induced CK2α kinase activity. A, the binding mode and docking score of LYG-202 on CK2α. B and C, effect of LYG-202 on TNF-α-induced CK2 activity and expression in HepG2 cells. Data are presented as means ± S.D. for at least three independent experiments performed in triplicate (*, $P < 0.05$; **, $P < 0.01$, compared with vehicle control).

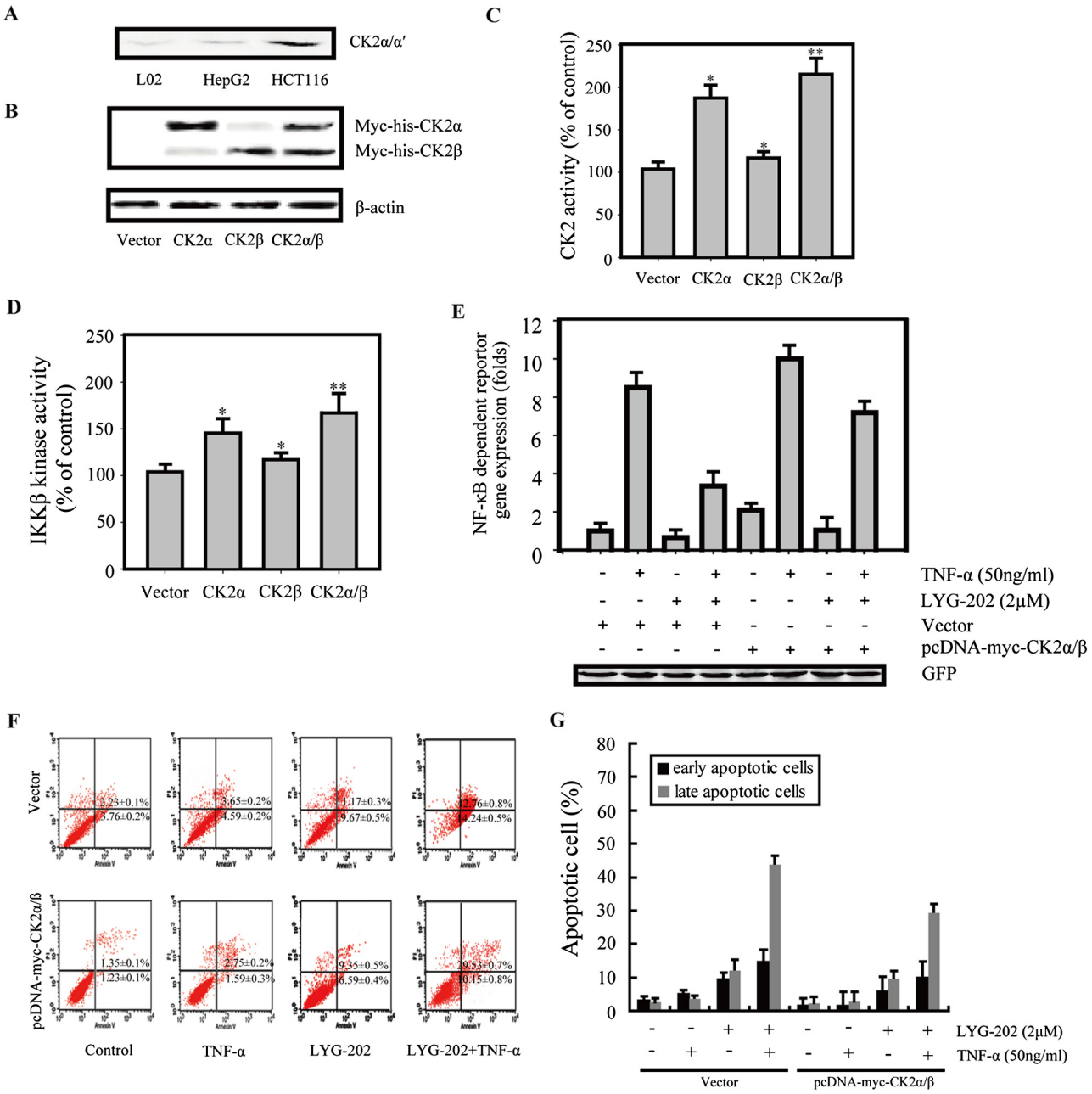

Fig. 6. Transfection of CK2 subunits diminished TNF-α-induced apoptosis. A, expression of CK2 in L02, HepG2, and HCT116 cells. B, transient overexpression of CK2 subunits in HepG2 cells. HepG2 cells were transfected with empty vector, Myc-His-tagged CK2α, and Myc-His-tagged CK2β or cotransfected with Myc-His-tagged CK2α plus Myc-His-tagged CK2β. Cell lysates were examined by Western blot using the monoclonal anti-Myc antibody. C and D, transient overexpression of CK2 subunits increases CK2 and downstream IKKβ activity. E, overexpression of CK2 subunits increased the NF-κB-dependent reporter gene expression induced by LYG-202. HepG2 cells were transiently cotransfected with the CK2 subunit plasmids along with a NF-κB luciferase reporter gene. F, cotransfection of CK2 subunits reduced the TNF-α-induced apoptosis. G, apoptosis rates of transfected HepG2 cells induced by TNF-α and its combination with LYG-202. Values are means ± S.D. for at least three independent experiments performed in triplicate.

compared with the scrambled control. The data in Supplemental Fig. 2, B and C, indicated that transfection of CK2 siRNA in HepG2 cells exhibiting a significant decrease in CK2 kinase activity produced lower levels of IKKβ kinase activity than in control cells.

Furthermore, transfection of CK2 siRNA mimics the effect of LYG-202 on NF-κB activation (Supplemental Fig. 2D) and TNF-α-induced cell apoptosis (Supplemental Fig. 2, E and F). These findings indicated that CK2 is a promising target of LYG-202 in suppression of NF-κB activation and plays a crucial role in the signal transduction that promotes cell growth and survival in HepG2 cells.

LYG-202 Inhibits Hepatoma Tumor Growth in the H_{22} Murine Tumor Model by Suppressing CK2 Activity and NF-κB-Mediated Antiapoptosis Protein Expression in the Presence of TNF-α In Vivo. On the basis of the results above, we proposed that LYG-202 sensitized hepatoma to TNF-α by attenuating CK2 and NF-κB activity. To demonstrate this hypothesis, we examined the effects of LYG-202 on the growth of H_{22} murine solid tumor and cell

apoptosis and CK2-dependent NF-κB activation with or without the administration of TNF-α in vivo.

The results were a decrease in tumor volume (Fig. 7A) and an increased inhibitory effect (Fig. 7B; Table 2) with the combination of LYG-202 (750, 500, 250, and 125 mg/kg) and TNF-α compared with the effects of LYG-202 or TNF-α alone, suggesting that treatment with LYG-202 and TNF-α together had more potential than that of either one alone in a mouse hepatoma H_{22} solid tumor model. As shown in Table 2, the CDI forLYG-202-treated groups (125 mg/kg) was smaller than 0.75, whereas the CDI for groups treated with LYG-202 (750, 500, and 250 mg/kg) combined with TNF-α were between 0.75 and 1, indicating that the combining LYG-202 (125 mg/kg) and TNF-α produces a significant synergistic effect.

To further discover whether LYG-202 potentiates cancer cell apoptosis induced by TNF-α in vivo, we stained the solid tumor sections with a TUNEL apoptosis staining kit. As shown in Fig. 7C, application of LYG-202 in the mouse tumor model significantly increased TNF-α-induced apoptosis in a dose-dependent manner. Furthermore, expression levels of the NF-κB-regulated antiapoptosis genes including Survivin, XIAP, Bcl-2, and Bcl-xL were significantly decreased (Fig. 7D) in vivo, and

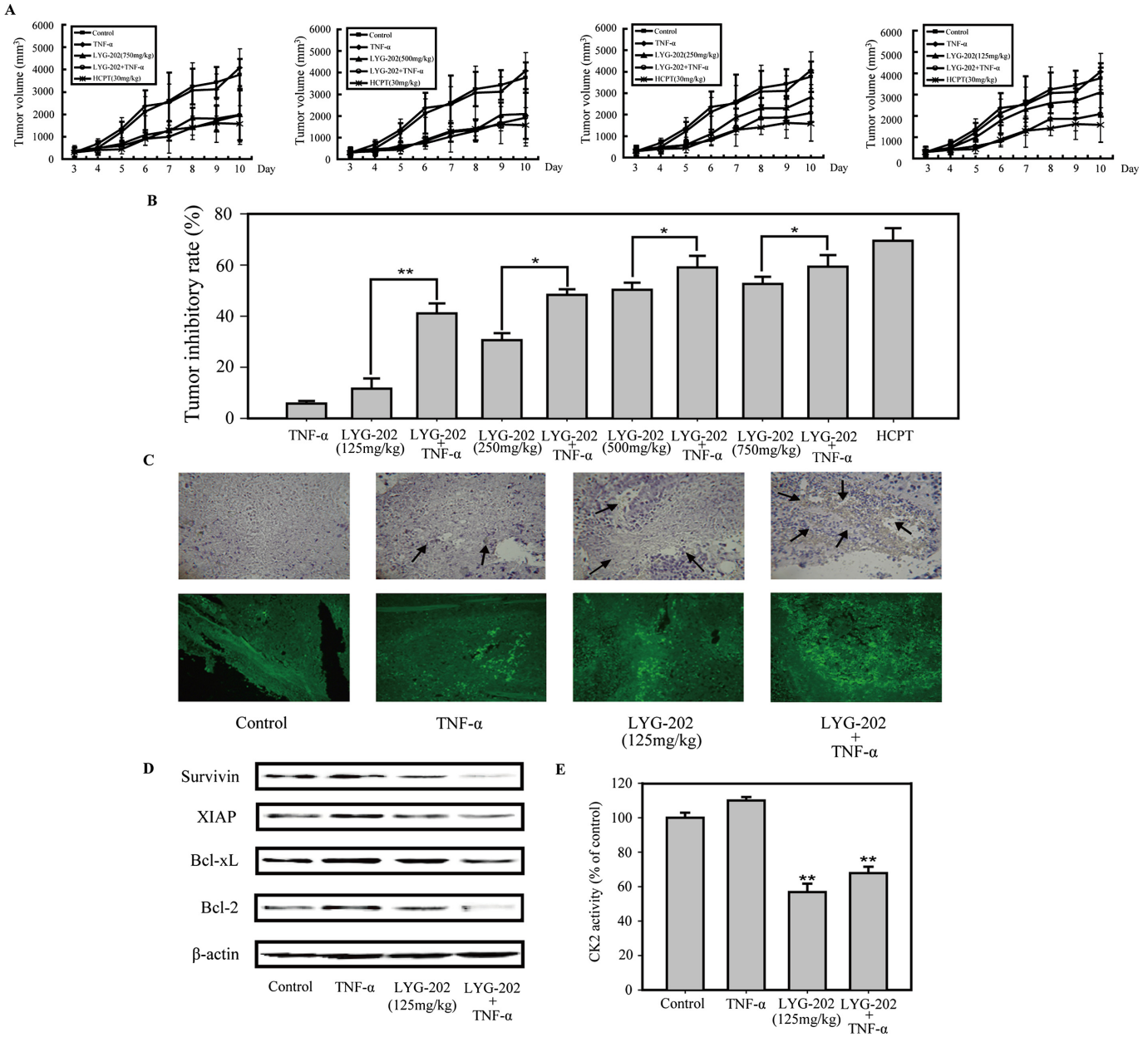

Fig. 7. LYG-202 suppresses H_{22} solid tumor growth, induces apoptosis, and inhibits CK2 activity and NF-κB-regulated antiapoptotic gene expression with the presence of TNF-α in vivo. A, LYG-202 inhibited H_{22} solid tumor growth in a xenograft mouse model at doses of 750, 500, 250, and 125 mg/kg with the administration of TNF-α (1.5 μg/day). Tumor volume significantly decreased with combination treatment of LYG-202 and TNF-α compared with that in the control group. B, inhibitory effect of LYG-202 alone or together with TNF-α on the growth of H_{22} murine solid tumor. Column, mean; bar, S.D. ($n = 3$; *, $P < 0.05$; **, $P < 0.01$, versus control). C, LYG-202 facilitated TNF-α-induced tumor apoptosis in a xenograft mouse model. Solid tumors were fixed and embedded with paraffin. The 0.5-mm sections were stained with a specific TUNEL staining kit (arrows indicate the TUNEL signals; original magnification, 100×). D, LYG-202 suppressed the expression levels of NF-κB-regulated antiapoptotic genes activated by TNF-α. E, LYG-202 quenched CK2 activity in the absence or presence of TNF-α in vivo. The results shown are representative of three independent experiments. Column, mean; bar, S.D. ($n = 3$; *, $P < 0.05$; **; $P < 0.01$ versus control).

TABLE 2
Summary of inhibitory effects of TNF-α and LYG-202 on H_{22} murine solid tumor

Groups	Incipient Body Weight	No. Animals	Telebody Weight	No. Animals	Tumor Weight	IR	CDI	Effect
	g		*g*		*g*	%		
Control	19.9 ± 0.9	10	22.5 ± 1.2	10	1.550 ± 0.110			
TNF-α, 1.5 μg/day	19.3 ± 0.5	10	23.8 ± 1.5	10	1.476 ± 0.252	4.78		
LYG-202								
750 mg/kg	20.9 ± 1.0	10	23.0 ± 1.0	10	0.718 ± 0.178**	53.65		
500 mg/kg	20.7 ± 0.9	10	22.7 ± 0.9	10	0.748 ± 0.195**	51.71		
250 mg/kg	18.5 ± 0.6	10	21.8 ± 1.0	10	1.053 ± 0.135*	32.04		
125 mg/kg	19.5 ± 1.0	10	23.5 ± 1.3	10	1.416 ± 0.228	8.61		
LYG-202 + TNF-α								
750 mg/kg+ 1.5 μg/day	19.7 ± 1.2	10	22.9 ± 1.2	10	0.621 ± 0.174**#	59.95	0.907	Synergistic
500 mg/kg + 1.5 μg/day	18.8 ± 0.6	10	24.0 ± 1.2	10	0.631 ± 0.155**#	59.29	0.885	Synergistic
250 mg/kg + 1.5 μg/day	21.0 ± 1.2	10	22.7 ± 0.9	10	0.820 ± 0.095**#	47.09	0.818	Synergistic
125 mg/kg + 1.5 μg/day	21.3 ± 0.9	10	24.5 ± 1.0	10	0.926 ± 0.125*##	40.28	0.686	Synergistic
HCPT, 30 mg/kg	20.3 ± 1.0	10	23.9 ± 1.1	10	0.478 ± 0.175**	69.18		

IR, inhibitory ratio of tumor weight.
* $P < 0.05$, compared with control.
** $P < 0.01$, compared with control.
$P < 0.01$.
# $P < 0.05$, combination compared with the LYG-202 (750, 500, 250, and 125 mg/kg) groups.

the decrease in CK2 activity (Fig. 7E) suggested that LYG-202 also had an inhibitory effect on CK2 activity in vivo. These results indicated that LYG-202 sensitized mouse hepatoma to TNF-α in the mouse H_{22} hepatoma tumor model.

Discussion

TNF-α is being used as an anticancer agent for locoregional treatment (Mocellin et al., 2005; Balkwill, 2009). However, its role in cancer therapy is debated because of its paradoxical activity: the caspase cascade for apoptosis induction and the NF-κB signal for cell survival promotion (Mocellin et al., 2005; van Horssen et al., 2006; Sethi et al., 2008). Thus, a good way to explore agents that enhance TNF-α-induced apoptosis is by attenuation of NF-κB activation. Molecular docking analysis and biological tests showed that LYG-202, a known synthesized flavonoid derivative, probably attenuated the NF-κB signal via inhibition of CK2 activity and may serve as a candidate compound for combination with TNF-α. In this study, we tested whether LYG-202 could sensitize hepatomas to treatment with TNF-α.

In human hepatoma HepG2 cells, which are reported to be resistant to TNF-α (Sugimoto et al., 1999), TNF-α alone had little effect on inhibition of proliferation and induction of apoptosis. Intriguingly, we even noticed that the cell fragment percentage slightly decreased compared with that for the control group. However, combination of TNF-α with LYG-202 significantly enhanced its antiproliferation and proapoptosis activities (Fig. 1). Previous studies showed that NF-κB is the major survival factor in preventing TNF-α-induced apoptosis, and inhibition of this transcription factor may improve the efficacy of apoptosis-inducing cancer therapies (Orlowski and Baldwin, 2002; Mocellin et al., 2005; van Horssen et al., 2006; Pilati et al., 2008; Balkwill, 2009). Our results indicated that the protein expression of NF-κB target genes including Survivin, XIAP, Bcl-2/Bcl-xL, c-Myc, COX-2, and cyclin D1 obviously decreased in the presence of LYG-202 (Fig. 2B), and further findings demonstrated that LYG-202 suppressed NF-κB transcription activity by disturbing the bond to its response elements (Fig. 3). We also found that LYG-202 inhibited TNF-α-induced phosphorylation and degradation of IκBα (Fig. 4C), a critical step for NF-κB translocation into the nucleus (Zandi et al., 1997), by attenuating IKKβ activity (Fig. 4D). All these observations suggested that LYG-202 enhanced TNF-α-induced apoptosis by weakening NF-κB activation.

CK2 is a highly conserved and ubiquitous serine/threonine kinase with a wide range of substrates involved in carcinogenesis and tumor progression (Litchfield, 2003; Yu et al., 2006). In addition, CK2 has been found to show increased protein expression levels and nuclear localization in cancer cells compared with those in their normal counterparts. These findings promote CK2 as an unfavorable prognostic marker in several cancers and consequently as a relevant therapeutic target (Prudent et al., 2010; Sun et al., 2010; Trembley et al., 2010). Recent studies report that CK2 contributes to aberrant NF-κB activation though enhancement of IKKβ activity for the phosphorylation of the Ser32/Ser36 NH_2 terminus of IκBα, a novel and distinct function from that of CK2 as a known COOH-terminal IKKβ (Yu et al., 2006; Brown et al., 2010). Inverse docking indicated that CK2 may be a potent target of LYG-202 in blocking of NF-κB activation. Molecular docking analysis showed that LYG-202 formed hydrogen bonds with Asn118 and Asp175, the key residues located in the hinge region and polar region, respectively, in the active site of CK2, indicating that LYG-202 could bind stably with CK2 (Fig. 5A). These results indicated that LYG-202 could be a potent and selective CK2 inhibitor and probably attenuate the CK2-mediated NF-κB signal. Here, we found that LYG-202 inhibited CK2 activity but had no effect on its protein level (Fig. 5, B and C), and overexpression of CK2 partially reversed the LYG-202 inhibitory effect on the TNF-α-induced DNA-binding activity of NF-κB in HepG2 cells (Fig. 6E). Moreover, the apoptotic cell percentage of HepG2 treated with TNF-α and LYG-202 was reduced in the presence of CK2α and CK2β subunits, which show continuously active CK2 activity (Fig. 6, F and G).

However, our studies showed that LYG-202 had little effect on NF-κB activation and apoptosis when CK2 expression was almost completely inhibited by transfection with CK2 siRNA (Supplemental Fig. 2A). The transfection of CK2 siRNA inhibited TNF-α-induced DNA-binding activity of NF-κB (Supplemental Fig. 2D), induced HepG2 cell apoptosis, and mimicked the apoptotic potential of LYG-202 combined with TNF-α (Supplemental Fig. 2, E and F). This evidence sug-

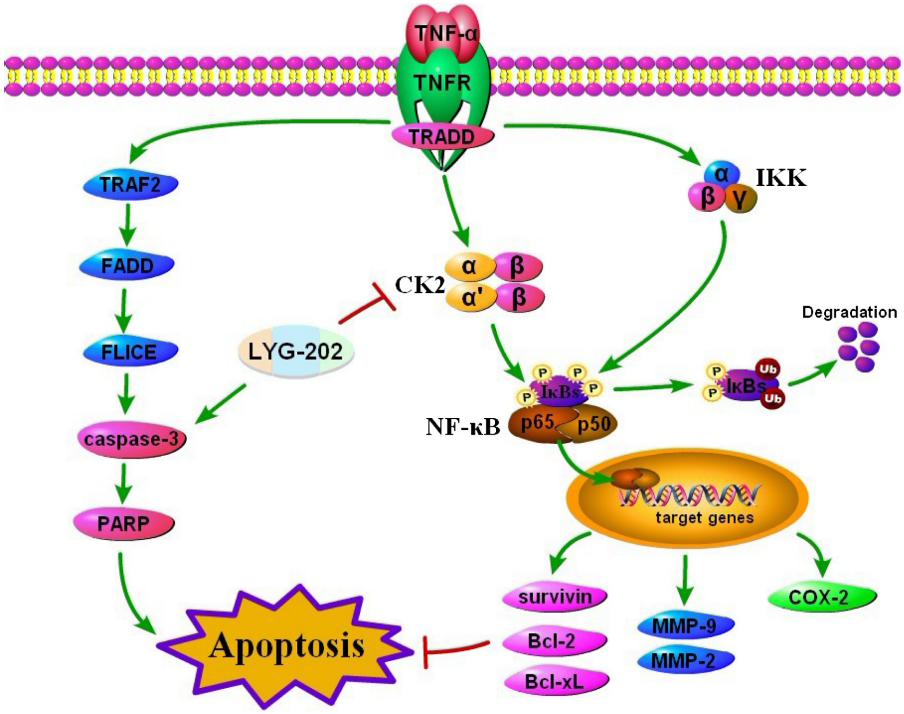

Fig. 8. A schematic diagram shows that LYG-202 enhances the antitumor activity of TNF-α by attenuating CK2-dependent NF-κB activation in HepG2 cells. Theoretically, LYG-202 or TNF-α alone can induce HepG2 cell death via a caspase-dependant apoptotic pathway. The apoptotic effect of TNF-α is blocked because of NF-κB-mediated antiapoptosis gene expression. LYG-202 can suppress NF-κB activation via its inhibition of CK2 activity and therefore enhances TNF-α-induced apoptosis. TRADD, TNFR-associated death domain protein; TRAF2, TNFR-associated factor 2; FADD, Fas associated protein with death domain.

gests that CK2 played a crucial role in signal transduction that promotes HepG2cell growth and survival and may serve as a target of LYG-202 for the promotional effect on TNF-α-induced apoptosis. Apigenin and other common flavonoids, which have been reported to be selective CK2 kinase inhibitors, suppress proliferation in a wide variety of solid tumors and hematological cancers (Davies et al., 2000; Zhao et al., 2011) and show significant inhibitory effects on CK2 activity and NF-κB activation (Farah et al., 2003). However, the possibility that LYG-202 could be a potent CK2 kinase inhibitor requires further assessment.

Increased tumor vessel permeability is currently believed to be critical for TNF-α antitumor activity. TNF-α improves the pharmacokinetic profile of coadministered drugs by increasing the permeability of tumor vessels and lowering interstitial pressure within the diseased tissue (Lejeune, 2002), which in turn augments the drug concentration within the tumor microenvironment (de Wilt et al., 2000; van der Veen et al., 2000). We found that LYG-202 exerted antiangiogenic activity both in vitro and in vivo (Chen et al., 2010b), which could be another explanation for the synergy between LYG-202 and TNF-α. Whether the effective contribution of TNF-α known to target tumor vasculature could promote the pro-apoptotic activity of LYG-202 needs to be investigated to fully realize its clinical potential.

Reactive oxygen species (ROS) generation in mitochondria is believed to play a key role in TNF-α-induced apoptosis (Schulze-Osthoff et al., 1992; Goossens et al., 1995). Previous studies have reported that LYG-202 induced HepG2 cell apoptosis through accumulation of ROS and its downstream signaling pathway (Chen et al., 2010a). Thus, the role of generation of ROS in HepG2 cell death induced by TNF-α combined with LYG-202 is worth further investigation.

A number of studies have shown that levels of TNF-α are elevated in the plasma of patients with alcoholic hepatitis (Bird et al., 1990; Miró et al., 1999). We found that LYG-202 with the combination treatment of TNF-α effectively suppressed H_{22} murine solid tumor growth, induced tumor apoptosis, and down-regulated anti-apoptosis genes in xenograft mouse models (Fig. 7). These results suggested that LYG-202 could be an effective agent in the treatment of patients with liver cancer with a high level of TNF-α secretion. However, whether the combination effect of LYG-202 with TNF-α in vivo occurs mainly via inhibition of CK2 activity should be further investigated, probably using a CK2α knockout mouse model.

In this study, we demonstrated that LYG-202 enhanced TNF-α-induced apoptosis via attenuation of CK2 activity, which leads to the abrogation of NF-κB activation in vitro and in vivo (Fig. 8). These results extended our understanding of the molecular mechanisms underlying the improvement in TNF-α antitumor activities by LYG-202.

Acknowledgments

We thank Dr. Stefania Sarno from the University of Padova for providing the plasmids of CK2α and CK2β.

Authorship Contributions

Participated in research design: Chen, Lu, and Guo.
Conducted experiments: Chen, Lu, Zhang, Zhao, He, and Sun.
Contributed new reagents or analytic tools: Sun and Li.
Performed data analysis: Chen, Lu, Zhang, Zhao, You, and Guo.
Wrote or contributed to the writing of the manuscript: Chen, Lu, Zhang, and Guo.

References

Aggarwal BB (2003) Signalling pathways of the TNF superfamily: a double-edged sword. *Nat Rev Immunol* **3:**745–756.
Balkwill F (2009) Tumour necrosis factor and cancer. *Nat Rev Cancer* **9:**361–371.
Bird GL, Sheron N, Goka AK, Alexander GJ, and Williams RS (1990) Increased plasma tumor necrosis factor in severe alcoholic hepatitis. *Ann Intern Med* **112:** 917–920.
Böcker W, Docheva D, Prall WC, Egea V, Pappou E, Rossmann O, Popov C, Mutschler W, Ries C, and Schieker M (2008) IKK-2 is required for TNF-α-induced invasion and proliferation of human mesenchymal stem cells. *J Mol Med* **86:**1183–1192.

Bosman FT, Visser BC, and van Oeveren J (1996) Apoptosis: pathophysiology of programmed cell death. *Pathol Res Pract* **192:**676–683.
Braun T, Carvalho G, Fabre C, Grosjean J, Fenaux P, and Kroemer G (2006) Targeting NF-κB in hematologic malignancies. *Cell Death Differ* **13:**748–758.
Brown MS, Diallo OT, Hu M, Ehsanian R, Yang X, Arun P, Lu H, Korman V, Unger G, Ahmed K, et al. (2010) CK2 modulation of NF-κB, TP53, and the malignant phenotype in head and neck cancer by anti-CK2 oligonucleotides in vitro or in vivo via sub-50-nm nanocapsules. *Clin Cancer Res* **16:**2295–2307.
Cao SS and Zhen YS (1989) Potentiation of antimetabolite antitumor activity in vivo by dipyridamole and amphotericin B. *Cancer Chemother Pharmacol* **24:**181–186.
Chen FH, Zhang LB, Qiang L, Yang Z, Wu T, Zou MJ, Tao L, You QD, Li ZY, Yang Y, et al. (2010a) Reactive oxygen species-mitochondria pathway involved in LYG-202-induced apoptosis in human hepatocellular carcinoma $HepG_2$ cells. *Cancer Lett* **296:**96–105.
Chen Y, Lu N, Ling Y, Wang L, You Q, Li Z, and Guo Q (2010b) LYG-202, a newly synthesized flavonoid, exhibits potent anti-angiogenic activity in vitro and in vivo. *J Pharmacol Sci* **112:**37–45.
Chou TC (2006) Theoretical basis, experimental design, and computerized simulation of synergism and antagonism in drug combination studies. *Pharmacol Rev* **58:**621–681.
Davies SP, Reddy H, Caivano M, and Cohen P (2000) Specificity and mechanism of action of some commonly used protein kinase inhibitors. *Biochem J* **351 (Pt 1):**95–105.
de Wilt JH, ten Hagen TL, de Boeck G, van Tiel ST, de Bruijn EA, and Eggermont AM (2000) Tumour necrosis factor α increases melphalan concentration in tumour tissue after isolated limb perfusion. *Br J Cancer* **82:**1000–1003.
Egberts JH, Cloosters V, Noack A, Schniewind B, Thon L, Klose S, Kettler B, von Forstner C, Kneitz C, Tepel J, et al. (2008) Anti-tumor necrosis factor therapy inhibits pancreatic tumor growth and metastasis. *Cancer Res* **68:**1443–1450.
Farah M, Parhar K, Moussavi M, Eivemark S, and Salh B (2003) 5,6-Dichloro-ribifuranosylbenzimidazole- and apigenin-induced sensitization of colon cancer cells to TNF-α-mediated apoptosis. *Am J Physiol Gastrointest Liver Physiol* **285:** G919–G928.
Goossens V, Grooten J, De Vos K, and Fiers W (1995) Direct evidence for tumor necrosis factor-induced mitochondrial reactive oxygen intermediates and their involvement in cytotoxicity. *Proc Natl Acad Sci USA* **92:**8115–8119.
Hayden MS and Ghosh S (2004) Signaling to NF-κB. *Genes Dev* **18:**2195–2224.
van Horssen R, Ten Hagen TL, and Eggermont AM (2006) TNF-α in cancer treatment: molecular insights, antitumor effects, and clinical utility. *Oncologist* **11:** 397–408.
Karin M and Ben-Neriah Y (2000) Phosphorylation meets ubiquitination: the control of NF-κB activity. *Annu Rev Immunol* **18:**621–663.
Kusaba M, Nakao K, Goto T, Nishimura D, Kawashimo H, Shibata H, Motoyoshi Y, Taura N, Ichikawa T, Hamasaki K, et al. (2007) Abrogation of constitutive STAT3 activity sensitizes human hepatoma cells to TRAIL-mediated apoptosis. *J Hepatol* **47:**546–555.
Lejeune FJ (2002) Clinical use of TNF revisited: improving penetration of anticancer agents by increasing vascular permeability. *J Clin Invest* **110:**433–435.
Li H, Zhu H, Xu CJ, and Yuan J (1998) Cleavage of BID by caspase 8 mediates the mitochondrial damage in the Fas pathway of apoptosis. *Cell* **94:**491–501.
Litchfield DW (2003) Protein kinase CK2: structure, regulation and role in cellular decisions of life and death. *Biochem J* **369 (Pt 1):**1–15.
Liu W, Dai Q, Lu N, Wei L, Ha J, Rong J, Mu R, You Q, Li Z, and Guo Q (2011) LYG-202 inhibits the proliferation of human colorectal carcinoma HCT-116 cells through induction of G_1/S cell cycle arrest and apoptosis via p53 and p21(WAF1/Cip1) expression. *Biochem Cell Biol* **89:**287–298.
Los M, Mozoluk M, Ferrari D, Stepczynska A, Stroh C, Renz A, Herceg Z, Wang ZQ, and Schulze-Osthoff K (2002) Activation and caspase-mediated inhibition of PARP: a molecular switch between fibroblast necrosis and apoptosis in death receptor signaling. *Mol Biol Cell* **13:**978–988.
Lu Z, Lu N, Li C, Li F, Zhao K, Lin B, and Guo Q (2012) Oroxylin A inhibits matrix metalloproteinase-2/9 expression and activation by up-regulating tissue inhibitor of metalloproteinase-2 and suppressing the ERK1/2 signaling pathway. *Toxicol Lett* **209:**211–220.
Manusama ER, Nooijen PT, Stavast J, Durante NM, Marquet RL, and Eggermont AM (1996) Synergistic antitumour effect of recombinant human tumour necrosis factor alpha with melphalan in isolated limb perfusion in the rat. *Br J Surg* **83:**551–555.
Middleton E Jr, Kandaswami C, and Theoharides TC (2000) The effects of plant flavonoids on mammalian cells: implications for inflammation, heart disease, and cancer. *Pharmacol Rev* **52:**673–751.
Miró F, Lelong JC, Pancetti F, Roher N, Duthu A, Plana M, Bourdon JC, Bachs O, May E, and Itarte E (1999) Tumour suppressor protein p53 released by nuclease digestion increases at the onset of rat liver regeneration. *J Hepatol* **31:**306–314.
Mocellin S, Rossi CR, Pilati P, and Nitti D (2005) Tumor necrosis factor, cancer and anticancer therapy. *Cytokine Growth Factor Rev* **16:**35–53.
Nakamura N, Hayasaka S, Zhang XY, Nagaki Y, Matsumoto M, Hayasaka Y, and Terasawa K (2003) Effects of baicalin, baicalein, and wogonin on interleukin-6 and interleukin-8 expression, and nuclear factor-κB binding activities induced by interleukin-1beta in human retinal pigment epithelial cell line. *Exp Eye Res* **77:**195–202.
Orlowski RZ and Baldwin AS, Jr. (2002) NF-κB as a therapeutic target in cancer. *Trends Mol Med* **8:**385–389.
Perez D and White E (2000) TNF-α signals apoptosis through a bid-dependent conformational change in Bax that is inhibited by E1B 19K. *Mol Cell* **6:**53–63.
Pfeffer K (2003) Biological functions of tumor necrosis factor cytokines and their receptors. *Cytokine Growth Factor Rev* **14:**185–191.
Pierre F, Chua PC, O'Brien SE, Siddiqui-Jain A, Bourbon P, Haddach M, Michaux J, Nagasawa J, Schwaebe MK, Stefan E, et al. (2011) Discovery and SAR of 5-(3-chlorophenylamino)benzo[*c*][2,6]naphthyridine-8-carboxylic acid (CX-4945), the first clinical stage inhibitor of protein kinase CK2 for the treatment of cancer. *J Med Chem* **54:**635–654.
Pilati P, Rossi CR, and Mocellin S (2008) Strategies to enhance the anticancer potential of TNF. *Front Biosci* **13:**3181–3193.
Prudent R, Sautel CF, and Cochet C (2010) Structure-based discovery of small molecules targeting different surfaces of protein-kinase CK2. *Biochim Biophys Acta* **1804:**493–498.
Schmid JA and Birbach A (2008) IκB kinase β (IKKβ/IKK2/IKBKB)—a key molecule in signaling to the transcription factor NF-κB. *Cytokine Growth Factor Rev* **19:**157–165.
Schoonbroodt S, Ferreira V, Best-Belpomme M, Boelaert JR, Legrand-Poels S, Korner M, and Piette J (2000) Crucial role of the amino-terminal tyrosine residue 42 and the carboxyl-terminal PEST domain of IκB α in NF-κB activation by an oxidative stress. *J Immunol* **164:**4292–4300.
Schulze-Osthoff K, Bakker AC, Vanhaesebroeck B, Beyaert R, Jacob WA, and Fiers W (1992) Cytotoxic activity of tumor necrosis factor is mediated by early damage of mitochondrial functions. Evidence for the involvement of mitochondrial radical generation. *J Biol Chem* **267:**5317–5323.
Sethi G, Sung B, and Aggarwal BB (2008) TNF: a master switch for inflammation to cancer. *Front Biosci* **13:**5094–5107.
Seynhaeve AL, de Wilt JH, van Tiel ST, Eggermont AM, and ten Hagen TL (2002) Isolated limb perfusion with actinomycin D and TNF-α results in improved tumour response in soft-tissue sarcoma-bearing rats but is accompanied by severe local toxicity. *Br J Cancer* **86:**1174–1179.
Siddiqui-Jain A, Drygin D, Streiner N, Chua P, Pierre F, O'Brien SE, Bliesath J, Omori M, Huser N, Ho C, et al. (2010) CX-4945, an orally bioavailable selective inhibitor of protein kinase CK2, inhibits prosurvival and angiogenic signaling and exhibits antitumor efficacy. *Cancer Res* **70:**10288–10298.
Sugimoto K, Shiraki K, Ito T, Fujikawa K, Takase K, Tameda Y, Moriyama M, and Nakano T (1999) Expression of functional CD40 in human hepatocellular carcinoma. *Hepatology* **30:**920–926.
Suk K, Lee H, Kang SS, Cho GJ, and Choi WS (2003) Flavonoid baicalein attenuates activation-induced cell death of brain microglia. *J Pharmacol Exp Ther* **305:**638–645.
Sun HP, Zhu J, Chen FH, and You QD (2010) Structure-based pharmacophore modeling from multicomplex: a comprehensive pharmacophore generation of protein kinase CK2 and virtual screening based on it for novel inhibitors. *Mol Informat* **30:**579–592.
Sung B, Pandey MK, Ahn KS, Yi T, Chaturvedi MM, Liu M, and Aggarwal BB (2008) Anacardic acid (6-nonadecyl salicylic acid), an inhibitor of histone acetyltransferase, suppresses expression of nuclear factor-κB-regulated gene products involved in cell survival, proliferation, invasion, and inflammation through inhibition of the inhibitory subunit of nuclear factor-κBα kinase, leading to potentiation of apoptosis. *Blood* **111:**4880–4891.
Trembley JH, Chen Z, Unger G, Slaton J, Kren BT, Van Waes C, and Ahmed K (2010) Emergence of protein kinase CK2 as a key target in cancer therapy. *Biofactors* **36:**187–195.
Uzzo RG, Leavis P, Hatch W, Gabai VL, Dulin N, Zvartau N, and Kolenko VM (2002) Zinc inhibits nuclear factor-kappa B activation and sensitizes prostate cancer cells to cytotoxic agents. *Clin Cancer Res* **8:**3579–3583.
van der Veen AH, de Wilt JH, Eggermont AM, van Tiel ST, Seynhaeve AL, and ten Hagen TL (2000) TNF-α augments intratumoural concentrations of doxorubicin in TNF-α-based isolated limb perfusion in rat sarcoma models and enhances antitumour effects. *Br J Cancer* **82:**973–980.
van Horssen R, Ten Hagen TL, and Eggermont AM (2006) TNF-α in cancer treatment: molecular insights, antitumor effects, and clinical utility. *Oncologist* **11:** 397–408.
Wallach D (1997) Cell death induction by TNF: a matter of self control. *Trends Biochem Sci* **22:**107–109.
Wang X, Zhang J, and Xu T (2008) Thioredoxin reductase inactivation as a pivotal mechanism of ifosfamide in cancer therapy. *Eur J Pharmacol* **579:**66–73.
Yu M, Yeh J, and Van Waes C (2006) Protein kinase casein kinase 2 mediates inhibitor-κB kinase and aberrant nuclear factor-κB activation by serum factor(s) in head and neck squamous carcinoma cells. *Cancer Res* **66:**6722–6731.
Zandi E, Rothwarf DM, Delhase M, Hayakawa M, and Karin M (1997) The IκB kinase complex (IKK) contains two kinase subunits, IKKα and IKKβ, necessary for IκB phosphorylation and NF-κB activation. *Cell* **91:**243–252.
Zeng S, Liu W, Nie FF, Zhao Q, Rong JJ, Wang J, Tao L, Qi Q, Lu N, Li ZY, et al. (2009) LYG-202, a new flavonoid with a piperazine substitution, shows antitumor effects in vivo and in vitro. *Biochem Biophys Res Commun* **385:**551–556.
Zhang LB, Qiang L, Chen FH, Wu T, Rong JJ, Zhao Q, Zou MJ, Yang Z, You QD, Li ZY, et al. (2010) DHF-18, a new synthetic flavonoid, induced a mitochondrial-mediated apoptosis of hepatocarcinoma cells in vivo and in vitro. *Eur J Pharmacol* **651:**33–40.
Zhao L, Chen Z, Wang J, Yang L, Zhao Q, Wang J, Qi Q, Mu R, You QD, and Guo QL (2010) Synergistic effect of 5-fluorouracil and the flavanoid oroxylin A on HepG2 human hepatocellular carcinoma and on H22 transplanted mice. *Cancer Chemother Pharmacol* **65:**481–489.
Zhao M, Ma J, Zhu HY, Zhang XH, Du ZY, Xu YJ, and Yu XD (2011) Apigenin inhibits proliferation and induces apoptosis in human multiple myeloma cells through targeting the trinity of CK2, Cdc37 and Hsp90. *Mol Cancer* **10:**104.

Address correspondence to: Dr. Qinglong Guo, State Key Laboratory of Natural Medicines, Jiangsu Key Laboratory of Carcinogenesis and Intervention, China Pharmaceutical University, 24 Tongjiaxiang, Nanjing 210009, China. E-mail: anticancer_drug@yahoo.com.cn